

**INFLUENCE OF TEMPERATURE ON CYCLIC FATIGUE  
RESISTANCE OF NICKEL-TITANIUM RECIPROCATING  
FILES**

**TAN TAT WAH**

**FACULTY OF DENTISTRY  
UNIVERSITY OF MALAYA  
KUALA LUMPUR**

**2019**

**INFLUENCE OF TEMPERATURE ON CYCLIC FATIGUE  
RESISTANCE OF NICKEL-TITANIUM RECIPROCATING  
FILES**

**TAN TAT WAH**

**RESEARCH REPORT SUBMITTED IN PARTIAL  
FULFILMENT OF THE REQUIREMENTS FOR THE  
DEGREE OF MASTER OF CLINICAL DENTISTRY  
(RESTORATIVE DENTISTRY IN CONSERVATIVE  
DENTISTRY)**

**FACULTY OF DENTISTRY  
UNIVERSITY OF MALAYA  
KUALA LUMPUR**

**2019**

**UNIVERSITY OF MALAYA**  
**ORIGINAL LITERARY WORK DECLARATION**

Name of Candidate: **Tan Tat Wah**  
Matric No: **DGI160003**  
Name of Degree: **Master of Clinical Dentistry (Restorative Dentistry in  
Conservative Dentistry)**  
Title of Research Report: **Influence of Temperature on Cyclic Fatigue Resistance  
of Nickel-Titanium Reciprocating Files**  
  
Field of Study: **Endodontics**

I do solemnly and sincerely declare that:

- (1) I am the sole author/writer of this Work;
- (2) This Work is original;
- (3) Any use of any work in which copyright exists was done by way of fair dealing and for permitted purposes and any excerpt or extract from, or reference to or reproduction of any copyright work has been disclosed expressly and sufficiently and the title of the Work and its authorship have been acknowledged in this Work;
- (4) I do not have any actual knowledge nor do I ought reasonably to know that the making of this work constitutes an infringement of any copyright work;
- (5) I hereby assign all and every rights in the copyright to this Work to the University of Malaya ("UM"), who henceforth shall be owner of the copyright in this Work and that any reproduction or use in any form or by any means whatsoever is prohibited without the written consent of UM having been first had and obtained;
- (6) I am fully aware that if in the course of making this Work I have infringed any copyright whether intentionally or otherwise, I may be subject to legal action or any other action as may be determined by UM.

Candidate's Signature

Date: 1<sup>st</sup> of November 2019

Subscribed and solemnly declared before,

Witness's Signature

Date: 1<sup>st</sup> of November 2019

Name:

Designation:

## ABSTRACT

**Aim:** To evaluate cyclic fatigue resistance of Reciproc Blue R25 and WaveOne Gold Primary at 20°C and 35°C.

**Material & Methods:** Cyclic fatigue resistance of rotary nickel-titanium instrument, Reciproc Blue R25 (VDW Dental, Munich, Germany) and WaveOne Gold Primary (Dentsply Maillefer, Baillagues, Switzerland) files were tested at 20°C and 35°C in a stainless steel artificial canal, with 60° angle of curvature and curvature radius of 5 mm. The instruments reciprocated freely within the stainless steel canal until fracture. Time between commencement of the rotation and file breakage was recorded. The length of the fractured fragments were noted. Two-way ANOVA was used to compare the length of the fractured fragments, the time to failure (in seconds) of same system between temperatures, and the time to failure of different system at the same temperature. The level of significance was set at  $\alpha=0.01$ .

**Results:** There were no statistically significant differences among the fracture length of separated instruments ( $p>0.05$ ). Reciproc Blue R25 showed a statistically significant reduction in fatigue life at 35°C compared with 20°C ( $p<0.001$ ) whereas WaveOne Gold Primary had no significant difference in cyclic fatigue resistance between the 2 temperatures tested ( $p>0.05$ ), Reciproc Blue R25 instruments exhibited a significantly higher resistance to cyclic fatigue than WaveOne Gold Primary instruments at both 20°C and 35°C ( $p<0.001$ ).

**Conclusion:** Cyclic fatigue resistance of Reciproc Blue is significantly reduced when the environmental temperature is increased from 20°C to 35°C. However, increasing environmental temperature from 20°C to 35°C does not affect the cyclic fatigue

resistance of WaveOne Gold. Reciproc Blue showed significant better cyclic fatigue resistance than WaveOne Gold at both 20°C and 35°C.

**Keywords:** Cyclic fatigue resistance, nickel-titanium, temperature, reciprocating

University of Malaya

## ABSTRAK

**Tujuan:** Untuk menilai rintangan keletihan kitaran Reciproc Blue R25 dan WaveOne Gold Primary pada 20°C dan 35°C.

**Bahan & Kaedah:** Rintangan keletihan kitaran untuk alat nikel-titanium yang berputar, iaitu Reciproc Blue R25 (VDW Dental, Munich, Germany) dan WaveOne Gold Primary (Dentsply Maillefer, Baillagues, Switzerland) diuji pada suhu 20°C dan 35°C dalam kanal tiruan keluli tahan karat, dengan sudut 60° kelengkungan dan jejari kelengkungan 5 mm. Alat-alat ini digunakan dalam kanal keluli tahan karat sehingga patah. Masa antara permulaan putaran dan pepatahan instrumen telah diambil. Panjang instrument yang patah telah direkodkan. Two-way ANOVA digunakan untuk membandingkan panjang instrumen yang patah, masa untuk mematah instrument (dalam saat) yang sama dalam suhu yang berlainan, masa untuk mematah sistem yang berbeza pada suhu yang sama. Tahap penting telah ditetapkan pada  $\alpha=0.01$ .

**Keputusan:** Tidak ada perbezaan yang ketara secara statistik di kalangan panjang instrumen yang dipatahkan ( $p>0.05$ ). Reciproc Blue R25 menunjukkan pengurangan ketara secara statistik dalam rintangan keletihan kitaran pada 35°C berbanding dengan 20°C ( $p<0.001$ ). Manakala, WaveOne Gold Primary tidak mempunyai perbezaan dalam rintangan keletihan kitaran di suhu 20°C dan 35°C ( $p>0.05$ ), Reciproc Blue R25 instrumen menunjukkan rintangan yang lebih tinggi secara statistik terhadap keletihan kitaran daripada instrumen WaveOne Gold Primary pada suhu 20°C dan 35°C ( $p<0.001$ ).

**Kesimpulan:** Rintangan keletihan kitaran Reciproc Blue berkurang apabila suhu persekitarannya meningkat dari 20°C hingga 35°C. Walau bagaimanapun, peningkatan suhu persekitaran dari 20°C hingga 35°C tidak mempengaruhi rintangan keletihan

kitaran WaveOne Gold. Reciproc Blue menunjukkan rintangan keletihan kitaran yang lebih baik daripada WaveOne Gold di suhu 20°C dan 35°C.

**Kata kunci:** Rintangan keletihan kitaran, nikel-titanium, suhu

University of Malaya

## ACKNOWLEDGEMENTS

First and foremost, I have to thank my research supervisors, Dr. Nora Sakina binti Mohd Noor, Associate Professor Dr. Mariam binti Abdullah and Dr. Asfand Ali Khan. Without their assistance and dedicated involvement in every step throughout the process, this research would have never been accomplished. Their invaluable help of constructive comments and suggestions throughout the experimental and research report have contributed to the success of this research.

Not forgotten, my appreciation to my engineering colleague, Mr. Tan Chee Hau who provided insight and expertise that greatly assisted the research. My acknowledgement also goes to all the technicians especially Mr. Haripin Bin Hassan, Mrs Zarina Binti Idris, Mr. Hassan Ismail and office staffs of Faculty of Dentistry for their co-operations.

I am grateful to Dr. Mahmoud Danaee, Dr. Shirley Hu Hui Hui, and Dr. Teo Chin Hai for their guidance on statistical analysis and report writing.

Sincere thanks to all my friends especially Dr. Lo Chai Ling, Dr. Lim Yee Ping, Dr. Muhammad Firdaus bin Mat Saad, Dr. Rana Abdelbaset Lofty Diab, Dr. Wael Ali Alawneh and others for their kindness and moral support during my study. To those who directly or indirectly contributed in this research, your kindness means a lot to me. Thank you very much.

My acknowledgement would be incomplete without thanking the biggest source of my strength, my family, particularly my parents and my wife, thank you for the love, support and encouragement throughout all stage in my life. Without you, I would not be the person I am today.



## TABLE OF CONTENTS

Abstract .....	iii
Abstrak .....	v
Acknowledgements .....	vii
Table of Contents .....	viii
List of Figures .....	xi
List of Tables.....	xiii
List of Symbols and Abbreviations.....	xiv
List of Appendices .....	xv
<b>CHAPTER 1: INTRODUCTION.....</b>	<b>1</b>
<b>CHAPTER 2: AIM &amp; OBJECTIVES OF STUDY.....</b>	<b>3</b>
2.1 Aim .....	3
2.2 Objectives of study .....	3
2.3 Null Hypothesis .....	3
<b>CHAPTER 3: LITERATURE REVIEW.....</b>	<b>4</b>
3.1 Introduction of Ni-Ti in Endodontics .....	4
3.2 Metallurgy.....	5
3.2.1 Crystal Characteristic of Ni-Ti .....	5
3.3 Failure of Ni-Ti.....	7
3.3.1 Cyclic Fatigue Fracture .....	7
3.3.2 Torsional Fracture .....	9
3.4 Factor Affecting Cyclic Fatigue Resistance .....	10
3.4.1 Temperature.....	10

3.4.2	Motion .....	11
3.4.3	Cross Section Area .....	12
3.4.4	Angle of Curvature and Radius of Curve .....	13
3.4.5	Surface Treatment of Ni-Ti Instrument.....	13
3.5	Method to Evaluate Cyclic Fatigue Resistance .....	14
3.5.1	Curved Glass and Metal Tube .....	14
3.5.2	Sloped Metal Block .....	16
3.5.3	3-point Bending with Stainless Steel Pins.....	17
3.5.4	Grooved Block-and-Rod .....	18
3.5.5	Stainless Steel Block with Artificial Canal .....	19
<b>CHAPTER 4: MATERIALS AND METHODS .....</b>		<b>22</b>
4.1	Sample Size Determination .....	22
4.2	Pilot Study .....	22
4.3	Cyclic Fatigue Resistance Test.....	23
4.4	Data Analysis.....	28
<b>CHAPTER 5: RESULTS.....</b>		<b>29</b>
5.1	Length of Fractured Tip.....	29
5.2	Time to Fracture .....	30
5.3	Mode of Fracture .....	33
<b>CHAPTER 6: DISCUSSION .....</b>		<b>36</b>
6.1	Methodology.....	36
6.2	Length .....	36
6.3	Time to Fracture.....	37
6.3.1	20°C vs 35°C .....	37

6.3.1.1	Reciproc Blue R25 .....	37
6.3.1.2	WaveOne Gold Primary .....	38
6.3.2	20°C and 35°C .....	38
6.4	Limitation .....	39
<b>CHAPTER 7: CONCLUSION &amp; RECOMMENDATION.....</b>		<b>40</b>
7.1	Conclusion .....	40
7.2	Recommendations.....	40
	References .....	41
	Appendix A: SEM of fractured surfaces.....	48

University of Malaya

## LIST OF FIGURES

Figure 3.1 Martensitic transformation and shape memory effect of Ni-Ti alloy when induced by stress and temperature (Thompson, 2000).....	5
Figure 3.2 SEM of fractured surface of instrument that caused by cyclic fatigue with crack initiation origin (arrows) and fast fracture zone (asterik) with dimples and fatigue striations (Hieawy <i>et al.</i> , 2015).....	8
Figure 3.3 SEM of fractured surface of instrument circular abrasion marks that caused by torsional fracture (Alcalde <i>et al.</i> , 2017). ....	9
Figure 3.4 Reciprocation motion (N. M. Grande <i>et al.</i> , 2015).....	12
Figure 3.5 An example of curved glass or metal tube to evaluate cyclic fatigue resistance (Plotino <i>et al.</i> , 2009b).....	15
Figure 3.6 An example of sloped metal block that used to evaluate cyclic fatigue resistance (Kitchens Jr <i>et al.</i> , 2007). ....	16
Figure 3.7 An example of 3-point Bending with Stainless Steel Pins (Cheung & Darvell, 2007a).....	17
Figure 3.8 An example of grooved block and rod (Haikel <i>et al.</i> , 1999).....	18
Figure 3.9 The V-groove for guiding the instrument (Haikel <i>et al.</i> , 1999).....	19
Figure 3.10 Metal block with 1.5 mm wide artificial canal (Larsen <i>et al.</i> , 2009). ....	20
Figure 3.11 An example of stainless steel block with artificial canal which reproduced the size and taper of instrument (Plotino <i>et al.</i> , 2009b). ....	21
Figure 4.1: (a) Stainless steel artificial canal which correspond to dimension of RB R25. (b) Stainless steel artificial canal which correspond to dimension of WG Primary. ....	23
Figure 4.2 (a) Shield. (b) Stainless steel canal. (c) Shield at the end of stainless steel canal. (d) Insertion of file. (e) Removal of shield. ....	24
Figure 4.3 Stainless steel canal in water bath. ....	24
Figure 4.4 Temperature of stainless steel canal monitored by digital laser infrared temperature sensor. ....	25
Figure 4.5 Digital Micro-caliper. ....	26
Figure 4.6 Flow chart of the research methodology. ....	27

Figure 5.1 SEM of RB R25 at 20°C with crack initiation origin (arrow) and fast fracture zone (asterik) with dimples and fatigue striations.....	33
Figure 5.2 SEM of RB R25 at 35°C with crack initiation origin (arrow) and fast fracture zone (asterik) with dimples and fatigue striations.....	34
Figure 5.3 SEM of WG Primary at 20°C with crack initiation origin (arrow) and fast fracture zone (asterik) with dimples and fatigue striations. ....	34
Figure 5.4 SEM of WG Primary at 35°C with crack initiation origin (arrow) and fast fracture zone (asterik) with dimples and fatigue striations. ....	35

University of Malaya

## LIST OF TABLES

Table 5.1 Mean and SD of length of fractured tip of RB R25 and WG Primary at 20°C and 35°C.....	29
Table 5.2 Normality test for length of fractured tip of RB and WG at 20°C and 35°C..	29
Table 5.3 Summary of Two-way ANOVA for temperature and type of instrument on length of fractured tip.....	30
Table 5.4 Mean and SD of time to fracture of RB R25 and WG Primary at 20°C and 35°C. ....	30
Table 5.5 Normality test for time to fracture of RB and WG at 20°C and 35°C. ....	31
Table 5.6 Summary of Two-way ANOVA for temperature and type of instrument on length of fractured tip.....	31
Table 5.7 The difference of time to fracture between levels of instruments for each level of temperature. ....	32
Table 5.8 The difference of time to fracture between levels of temperatures for each level of instrument.....	32

## LIST OF SYMBOLS AND ABBREVIATIONS

°C	:	Degree Celsius
A <sub>f</sub>	:	Austenite finish temperature
A <sub>s</sub>	:	Austenite transformation start temperature
M <sub>f</sub>	:	Martensite finish temperature
mm	:	Milimetre
NCF	:	Number of cycles to fracture
Ni-Ti	:	Nickel titanium
RB	:	Reciproc Blue
s	:	Second
SD	:	Standard deviation
SEM	:	Scanning electron microscope
TtF	:	Time to fracture
WG	:	WaveOne Gold

## LIST OF APPENDICES

Appendix A: SEM of fractured surfaces

48-49

University of Malaya



## CHAPTER 1: INTRODUCTION

Nickel-titanium (Ni-Ti) rotary instruments have been widely used for root canal preparation. However, they have a tendency to fracture unpredictably due to cyclic fatigue which will occur without any sign of a previous permanent plastic deformation (Plotino *et al.*, 2009b). The cyclic fatigue fracture is the result of the alternating tension-compression cycles of the instrument when it flexed in the region of maximum curvature of the canal (Sattapan *et al.*, 2000).

Various manufacturing strategies for Ni-Ti rotary endodontic files have been developed to improve flexibility and resistance to fatigue fracture. These include different cross-sectional designs, the use of new alloys that provide superior mechanical properties (flexibility, resistance to fatigue fracture) and improvement in the manufacturing process (Gambarini *et al.*, 2008; Gambarini *et al.*, 2012; Plotino *et al.*, 2012)

Recently, manufacturers have introduced several thermally treated Ni-Ti to optimize the microstructure and transformation behaviour of Ni-Ti alloys. This has improved mechanical properties of Ni-Ti files such as fatigue resistance to prolong the life span of Ni-Ti rotary instrument (Lopes *et al.*, 2013; Pereira *et al.*, 2013; Pérez-Higueras *et al.*, 2013; Shen *et al.*, 2012). A new generation of instruments such as Vortex Blue and ProTaper Gold rotary files by Dentsply Tulsa Dental Specialties undergo a complex heating-cooling proprietary treatment that results in a visible titanium oxide layer in the surface of the instrument. This treatment controls the transition temperatures, creating a shape memory alloy, which is claimed by the manufacturer as having superior mechanical properties and performance (Hieawy *et al.*, 2015; Plotino *et al.*, 2014; Silva *et al.*, 2016).

A new reciprocating motion was introduced by Yared (2008) and this motion can extend the life span of a Ni-Ti instrument by improving its cyclic fatigue resistance of instrument as compared to continuous rotation movement (Gavini *et al.*, 2012; Pedullà *et al.*, 2018). In reciprocating movement, the instruments travel a shorter angular distance than rotary instruments because it will rotate opposite direction to reduce the stress accumulate on the instruments. Therefore, the reciprocating instrument will be subjected to lower stress values, resulting in an extended fatigue life (De-Deus *et al.*, 2010; Kiefner *et al.*, 2014; Pedullà *et al.*, 2013). Reciproc (VDW, Munich, Germany) and WaveOne (Dentsply Maillefer, Baillagues, Switzerland) are the main examples of commercially available systems for root canal preparation using reciprocating motion.

According to a review of the literature, there is limited study which compare the cyclic fatigue resistance of Reciproc Blue (RB) and WaveOne Gold (WG) instruments especially between different temperatures. This research will add valuable information to the literature as so far no study has been conducted that analyses and compares the cyclic fatigue resistance of these two instruments at room and intra-canal temperature.

## **CHAPTER 2: AIM & OBJECTIVES OF STUDY**

### **2.1 Aim**

The aim of this study is to evaluate cyclic fatigue resistance of Reciproc Blue R25 and WaveOne Gold Primary at 20°C and 35°C.

### **2.2 Objectives of study**

- To compare cyclic fatigue resistance of Reciproc Blue R25 between 20°C and 35°C.
- To compare cyclic fatigue resistance of WaveOne Gold Primary between 20°C and 35°C.
- To compare cyclic fatigue resistance of Reciproc Blue R25 and WaveOne Gold Primary at 20°C and 35°C.

### **2.3 Null Hypothesis**

- There is no different in cyclic fatigue resistance of Reciproc Blue R25 and WaveOne Gold Primary at 20°C and 35°C.

## CHAPTER 3: LITERATURE REVIEW

### 3.1 Introduction of Ni-Ti in Endodontics

Ni-Ti alloy was developed by the Naval Ordnance Laboratory (White Oak, MD, USA) (Buehler *et al.*, 1963). It was named Nitinol; an acronym for nickel (ni), titanium (ti) and Naval Ordnance Laboratory (nol). The properties of Ni-Ti alloy are shape-memory, super-elasticity, corrosion resistance and biocompatibility. Since Walia *et al.* (1988) introduced the use of Ni-Ti alloys for endodontic instruments, it has been widely used for root canal preparation.

Procedural errors during canal preparation such as zips, ledges, strip perforations or canal transportations can occur in both stainless steel and Ni-Ti endodontic instruments. It has been proved that root canal preparation with rotary Ni-Ti endodontic instruments leads to significantly less canal transportation and fewer procedural errors compared to stainless steel hand instruments (Schäfer, 2001). However, Ni-Ti instruments have a tendency to fracture unpredictably due to torsional fatigue and cyclic fatigue which can occur without any signs of previous permanent plastic deformation (Plotino *et al.*, 2009b). Torsional fracture happens when the tip of the instrument binds within the canal whilst the shank keeps turning resulting in the elastic limit of the Ni-Ti endodontic instrument being exceeded (Peters & Barbakow, 2002). The cyclic fatigue fracture is the result of alternating tension-compression cycles of the instrument when it is flexed at the region of maximum curvature of the canal (Sattapan *et al.*, 2000). Instrument separation will compromise the prognosis of root canal treatment if the canal is not properly disinfected (Simon *et al.*, 2008).

## 3.2 Metallurgy

### 3.2.1 Crystal Characteristic of Ni-Ti

Ni-Ti alloy used in endodontic instruments contain approximately 56% nickel and 44% titanium by weight, resulting in a nearly one-to-one atomic ratio (Thompson, 2000). Ni-Ti alloy can exist in two different temperature-dependent crystal structures named austenite (high-temperature or parent phase) and martensite phase (low-temperature phase) (Shen *et al.*, 2013). Austenite phase can transform into martensite phase when induced by stress or temperature and vice versa (Figure 3.1).

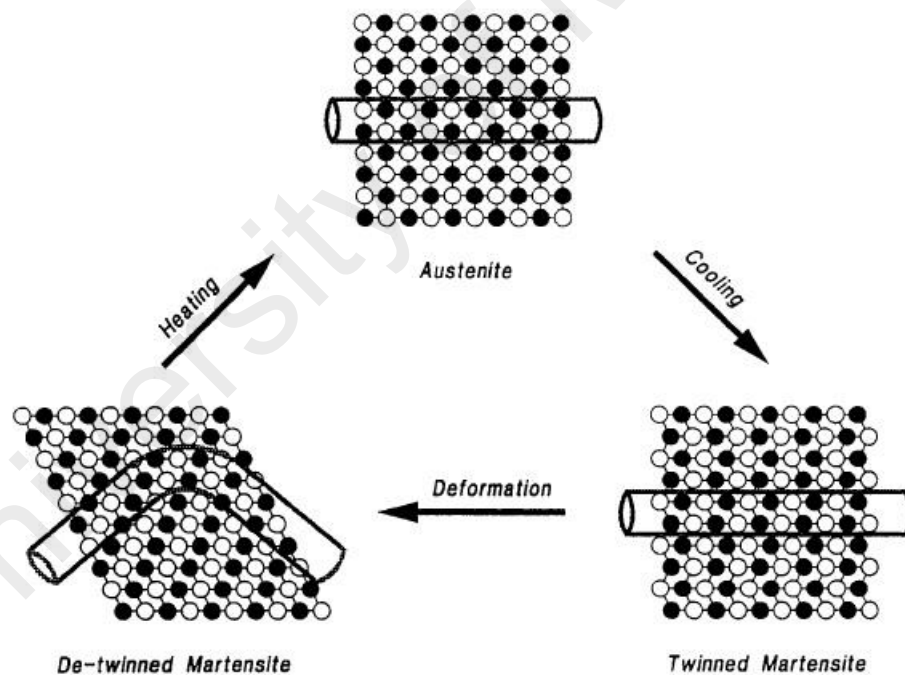


**Figure 3.1** Martensitic transformation and shape memory effect of Ni-Ti alloy when induced by stress and temperature (Thompson, 2000).

The properties of alloy is depending on the ambient temperature and austenite finish temperature ( $A_f$ ) of the alloy.  $A_f$  is defined as the critical finishing temperature for the martensite to completely transform into austenite on heating (McCormick *et al.*, 1993). The alloy will be in austenite phase and possess superior superelastic properties if the ambient temperature is above  $A_f$  (Zhou *et al.*, 2013). According to Kuhn and Jordan (2002), austenite has higher elastic modulus than martensite and R-phase has the lowest elastic modulus. When the material is in its austenitic form, it is quite strong and hard.

The Ni-Ti alloy is in martensitic state if the ambient temperature is below martensite finish temperature ( $M_f$ ). The alloy will be soft, ductile, easily be deformed and possesses the shape memory effect (Zhou *et al.*, 2013). Ni-Ti alloy which in martensite phase possess superior cyclic fatigue resistance compared to austenite phase (Shen *et al.*, 2013).

In 2011, Dentsply Tulsa Dental (Tulsa, OK, USA) introduced ProFile Vortex Blue, which was the first endodontic instrument possessing a distinctive blue colour due to the visible titanium oxide layer on the surface of the instrument. ProFile Vortex Blue has significant better cyclic fatigue resistance than ProTaper Universal in both room and body temperature (Vasconcelos *et al.*, 2016). RB (VDW Dental, Munich, Germany) and WG (Dentsply Maillefer, Baillagues, Switzerland) are two heat-treated Ni-Ti systems which similar to ProFile Vortex Blue but rotates in reciprocating motion. These instruments possess controlled memory effect and can be pre-bend at room temperature (Plotino *et al.*, 2014).

The  $A_f$  of ProTaper Gold is approximately 50°C (Hieawy *et al.*, 2015). Thus, these instruments also mainly contain martensite or R-phase under clinical conditions. All Gold and Blue heat-treated files demonstrated superior flexibility and fatigue resistance

compared to conventional Ni-Ti and M-Wire instruments (De-Deus *et al.*, 2017; Gao *et al.*, 2012; Hieawy *et al.*, 2015) which can be attributed to their martensitic state.

### **3.3 Failure of Ni-Ti**

#### **3.3.1 Cyclic Fatigue Fracture**

Cyclic fatigue fracture occurs when the instrument rotates freely in a curvature, generating tension/compression cycles at the point of maximum flexure until the fracture occurs. As an instrument is held in a static position and continues to rotate, one half of the instrument shaft on the outside of the curve is in tension, whereas the half of the shaft on the inside of the curve is in compression. This repeated tension-compression cycle, caused by rotation within curved canals, will lead to instrument fracture (Peters, 2004).

Peng *et al.* (2005) collected 122 discarded ProTaper S1 from an endodontic clinic in 17 months and examined the instrument under scanning electron microscope (SEM). They classified most of the fractured instrument as flexural failure. This implies that fatigue is the predominant mechanism for instrument failure. Cheung *et al.* (2005) also reported that a great majority (93%) of instruments have failed because of flexural fatigue after they examined 28 fractured ProTaper S1 instrument discarded by an endodontic clinic at a stomatological school in China under a SEM.

The total cyclic life of Ni-Ti endodontic instruments can be divided into two stages: First is crack initiation in which micro-cracks form and start to grow preferentially along specific crystallographic planes or grain boundaries followed by crack propagation until final fracture (Gao *et al.*, 2010). Cyclic fatigue resistance is usually measured by the time until a fracture occurs or by the number of cycles to fracture

(NCF). However, Fidler (2014) reported that the NCF cannot be rigorously determined for reciprocating files revolving in both clockwise and counterclockwise directions. Thus, the time to fracture has been used in the recent studies to evaluate the fatigue life of files instead of the NCF (Keskin *et al.*, 2017; Klymus *et al.*, 2018; Plotino *et al.*, 2018).

Under SEM, fatigue striations left on the fractured surface by the incremental progression of a crack are unique to cyclic fatigue fracture (Figure 3.2); these striation marks can only be observed on cross sectional surface of the fractured instrument.

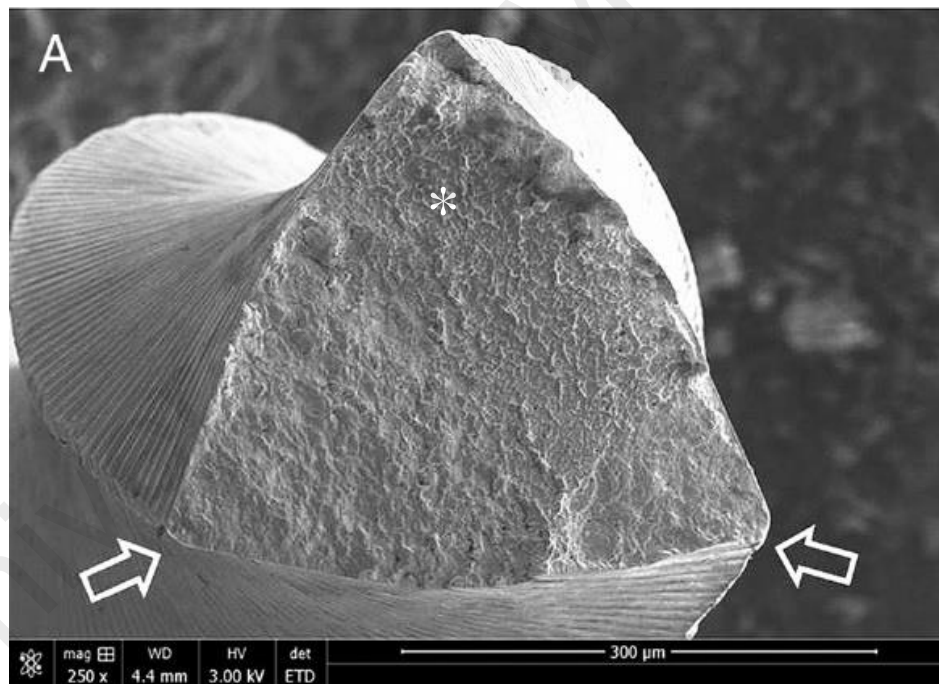


**Figure 3.2 SEM of fractured surface of instrument that caused by cyclic fatigue with crack initiation origin (arrows) and fast fracture zone (asterisk) with dimples and fatigue striations (Hieawy *et al.*, 2015).**



### 3.3.2 Torsional Fracture

Torsional fracture happens when the tip or another part of the instrument binds within the canal whilst the shank keeps turning resulting in the elastic limit of the Ni-Ti endodontic instrument being exceeded (Peters & Barbakow, 2002). It can happen in straight or curved canals, especially in the narrow and constricted canals (Sattapan *et al.*, 2000).

Fractography of torsional fracture is characterized by circular abrasion marks on the fractured surface (Figure 3.3). The skewed dimples are the typical of ductile failure of metals due to excess monotonic shear stress near the center of the fracture surface.



**Figure 3.3 SEM of fractured surface of instrument circular abrasion marks that caused by torsional fracture (Alcalde *et al.*, 2017).**

### 3.4 Factor Affecting Cyclic Fatigue Resistance

#### 3.4.1 Temperature

There are numerous studies which use different experimental design and testing models to evaluate the cyclic fatigue resistance of Ni-Ti instruments. However, the majority of those studies conducted the experiment at room temperature (Adıgüzel & Capar, 2017; Gündoğar & Özyürek, 2017; Higuera *et al.*, 2015; Keskin *et al.*, 2017). de Hemptinne *et al.* (2015) confirmed that the intra-canal temperature is 35°C ( $\pm 1.0^\circ\text{C}$ ) in an *in vivo* study and it is much higher than room temperature. The effect of temperature on cyclic fatigue resistance of rotary Ni-Ti instruments was proven by de Vasconcelos *et al.* (2016) who increase the environmental temperature from room temperature to intracanal temperature and found that cyclic fatigue resistance was significantly reduced at higher temperature. This result is confirmed by Dosanjh *et al.* (2017) who revealed that an increased in ambient temperature from 3°C to 60°C will result in significant reduction in cyclic fatigue of Ni-Ti rotary files regardless the brand of Ni-Ti instruments.

Mechanical properties of Ni-Ti instruments are determined by their phase transformation temperatures and ambient temperature during testing (Plotino *et al.*, 2017). Several studies reported that martensitic alloys are more fatigue resistant than austenitic instruments (Nguyen *et al.*, 2014; Plotino *et al.*, 2014). Instruments with  $A_f$  temperature between the room and intracanal temperature will have lower cyclic fatigue resistance at the intracanal temperature (de Vasconcelos *et al.*, 2016) due to the alloy being completely in austenite phase.

For example, the  $A_f$  temperature of ProTaper Gold F2 is 50°C (Hieawy *et al.*, 2015). Hence, the ProTaper Gold F2 will remain in martensite phase even when the testing temperature at intracanal temperature. However, the  $A_f$  temperature of ProTaper

Universal F2 (Dentsply Maillefer, Ballaigues, Switzerland) is 21°C and it is in austenitic phase at intracanal temperature. Consequently, the cyclic fatigue resistance of ProTaper Gold is significantly higher than ProTaper Universal at intracanal temperature (Hieawy *et al.*, 2015).

### 3.4.2 Motion

Traditionally, rotary Ni-Ti instruments operate with continuous rotating motion. Yared (2008) incorporated reciprocating motion on Ni-Ti instrument in order to introduce single use and single file system. Reciprocating motion can be described as an oscillating motion when an instrument rotates in 1 direction and then reverses direction before completing a full rotary cycle (Wan *et al.*, 2011) (Figure 3.4). According to the manufacturers, the setting on the endodontic motor, 'Wave-One ALL' mode generates a rotation of 170° CCW and 50° CW, and the 'Reciproc ALL' mode generates a rotation of 150° CCW and 30° CW (Kim *et al.*, 2012). The reciprocating movement derived from the principle of "Balanced Forces" by Roane *et al.* (1985).

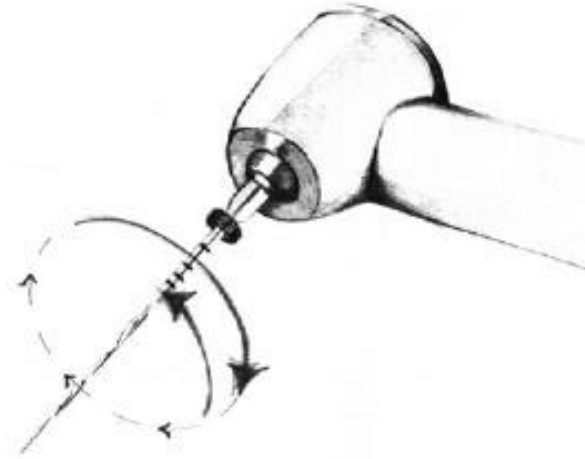


**Figure 3.4 Reciprocation motion (N. M. Grande *et al.*, 2015).**

Kiefner *et al.* (2014) conducted a study to compare the cyclic fatigue resistance of Reciproc and Mtwo (VDW, Munich, Germany) in reciprocating and continuous rotary motion. They found out that the reciprocation motion significantly enhanced the cyclic fatigue resistance of Ni-Ti instruments when compared to continuous rotating motion. This finding is consistent with Pedullà *et al.* (2013) and Pérez-Higueras *et al.* (2013). This might be due to the fact that reciprocating movement will ensure that the instruments always work below the elastic limit (Kim *et al.*, 2012).

### **3.4.3 Cross Section Area**

de Melo *et al.* (2002) compared the cyclic fatigue resistance of Profile (Tulsa Dental Products, Tulsa, OK) and Quantec (Tycon Inc., Chattanooga, TN) and they concluded that the size of instrument will affect the cyclic fatigue resistance of rotary Ni-Ti instrument instead of the design of the cutting flutes. This finding is confirmed by Grande *et al.* (2006) who compared different sizes of ProTaper Universal and Mtwo.

They concluded that the larger metal mass at the point of maximum stress, the shorter the lifespan of a Ni–Ti rotary instrument.

Uygun *et al.* (2016) compared the cyclic fatigue resistance of ProTaper Gold, ProTaper Next and ProTaper Universal at 5mm and 8mm from the tip of instruments. All instruments have better cyclic fatigue resistance at 5mm from the tip than 8mm from the tip. These results concluded that the smaller the cross section area of the instruments, the better the cyclic fatigue resistance of Ni-Ti instruments.

#### **3.4.4 Angle of Curvature and Radius of Curve**

Pruett *et al.* (1997) compared the cyclic fatigue resistance of Lightspeed instruments (Lightspeed Technologies, Inc., San Antonio, TX) by rotating the instrument in a metal tube with angles of curvature of 30°, 45°, or 60°, and radii of curvature of 2 mm or 5 mm. They found out that increase in severity of angle of curvature and/or reduction in the radius of the curve will decrease instrument lifespans. This result was consistent with Grande *et al.* (2006) who evaluate the cyclic fatigue resistance of ProTaper Universal and Mtwo with stainless steel artificial canals which had radii of curvature of 2 mm or 5 mm and an angle of curvature of 60°. Thus, the cyclic fatigue resistance of rotary Ni-Ti instruments is influenced by angle of curvature and radius of curve.

#### **3.4.5 Surface Treatment of Ni-Ti Instrument**

Some studies found that metal surface modification can improve the physical properties such as surface hardness, wear resistance, cyclic fatigue resistance of Ni-Ti instrument (Anderson *et al.*, 2007; Jabbari *et al.*, 2012; Praisarnti *et al.*, 2010). In the

literature, there are numerous Ni-Ti surface treatment that are utilised by manufacturers to extend the lifespan of Ni-Ti instruments. Examples are electropolishing (Cheung *et al.*, 2007), ion-implantation (Wolle, *et al.*, 2009), titanium nitride techniques using physical vapor deposition (Gavini *et al.*, 2010), thermal nitriding (Rapisardaa *et al.*, 2000) and metal organic chemical vapor deposition (Tripi *et al.*, 2002). However, some studies found surface treatment do not significantly increase the cyclic fatigue resistance of Ni-Ti instruments (Barbosa *et al.*, 2008; Cheung *et al.*, 2007,).

### **3.5 Method to Evaluate Cyclic Fatigue Resistance**

Various designs have been used to evaluate cyclic fatigue resistance of rotary Ni-Ti instruments, however, to the present time, there has been no standardization of cyclic fatigue resistance test.

#### **3.5.1 Curved Glass and Metal Tube**

Some authors have tested rotary Ni-Ti instruments in a curved cylindrical glass tube (Anderson *et al.*, 2007) or metal tube (Lopes *et al.*, 2007; Pruett *et al.*, 1997) to simulate canal with different diameters and point of maximum curvature and using different radii and angles of curvature (Figure 3.5).

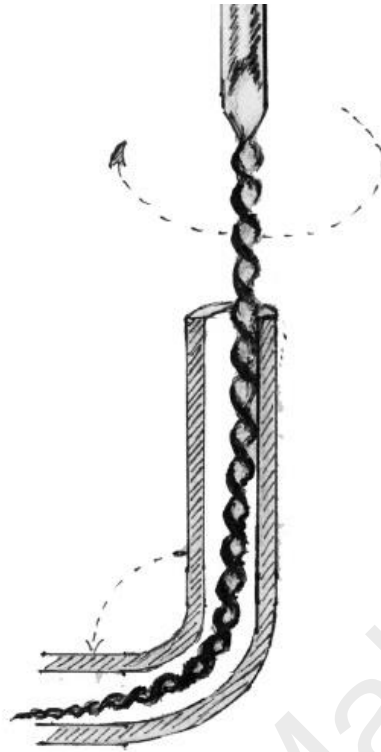


**Figure 3.5 An example of curved glass or metal tube to evaluate cyclic fatigue resistance (Plotino *et al.*, 2009b).**

However, cylindrical tubes cannot restrict the instrument shaft, thus the instrument will spring back into its original straight shape and reduce the curvature of instrument in the tube. Besides, the inner diameter of the tubes (glass and metal) is greater than the testing instruments and this will cause the rotating instrument to follow a trajectory which is not predictable and not follow the parameters of radius and angle of curvature and point of maximum curvature that were established when constructing the artificial canals.

### 3.5.2 Sloped Metal Block

Several studies have used high hardness sloped metal block with groove to evaluate cyclic fatigue of rotary Ni-Ti instruments (Kitchens Jr *et al.*, 2007; Li *et al.*, 2002; Ray *et al.*, 2007). The function of the groove is to keep the file in place during testing (Figure 3.6). However, this method is not recommended because it is unclear if a groove is able to constrain the tiny tip of an endodontic instrument during the test. If the tip of instrument is not placed precisely, it would not have a precise trajectory and the direct comparison between instruments of different brands may be difficult.

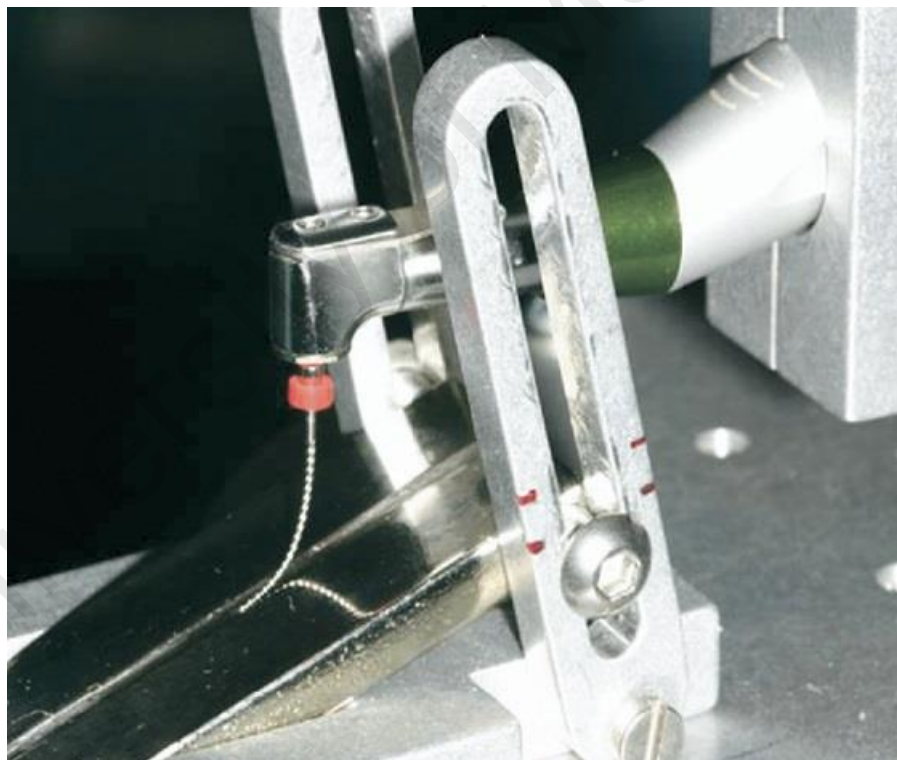


**Figure 3.6** An example of sloped metal block that used to evaluate cyclic fatigue resistance (Kitchens Jr *et al.*, 2007).



### 3.5.3 3-point Bending with Stainless Steel Pins

Cheung and Darvell (2007b) advocated a 3-point bending technique which used three smooth cylindrical stainless steel pins with high hardness to constrain the rotary Ni-Ti instruments during evaluation of the cyclic fatigue resistance (Figure 3.7). A small V-shaped groove was prepared on the lowest pin to maintain the position of the tip during rotation. The position of the pins will determine the curvature of the rotary Ni-Ti instrument during the test. Hieawy *et al.* (2015) and de Vasconcelos *et al.* (2016) used this technique to evaluate the cyclic fatigue resistance of rotary Ni-Ti instruments.



**Figure 3.7 An example of 3-point Bending with Stainless Steel Pins (Cheung & Darvell, 2007a).**

### 3.5.4 Grooved Block-and-Rod

Some studies (Haikel *et al.*, 1999; Tripi *et al.*, 2006) have used an artificial canal with a grooved concave tempered steel block and a convex tempered steel cylinder, which when held and fixed together, guaranteed the curve of the instruments (Figure 3.8). The concave radius block incorporated a notched V-form for guiding the instruments and was constructed with different radii and angles of curvature (Figure 3.9).

However, there has been no mention of the fit of the instrument in the block-and-rod assembly. The convex cylinder contacts the tapered instrument in a non-predictable way, so that the instrument may fit loosely and radius and angle of curvature may not be repeatable. Furthermore, it is difficult to control exactly the depth of the instrument in these devices so that the point of the instrument, which lies in the center of the curvature, may vary.

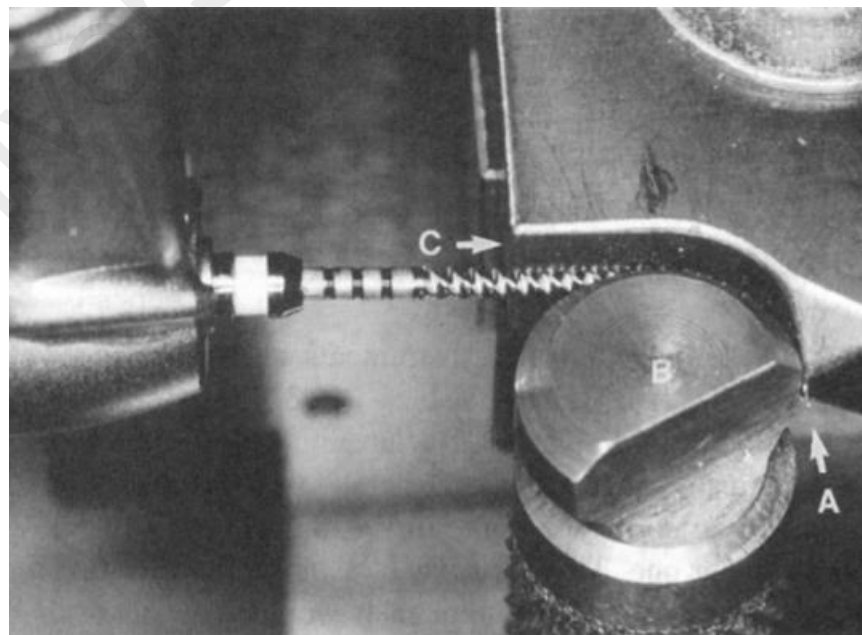


**Figure 3.8** An example of grooved block and rod (Haikel *et al.*, 1999).

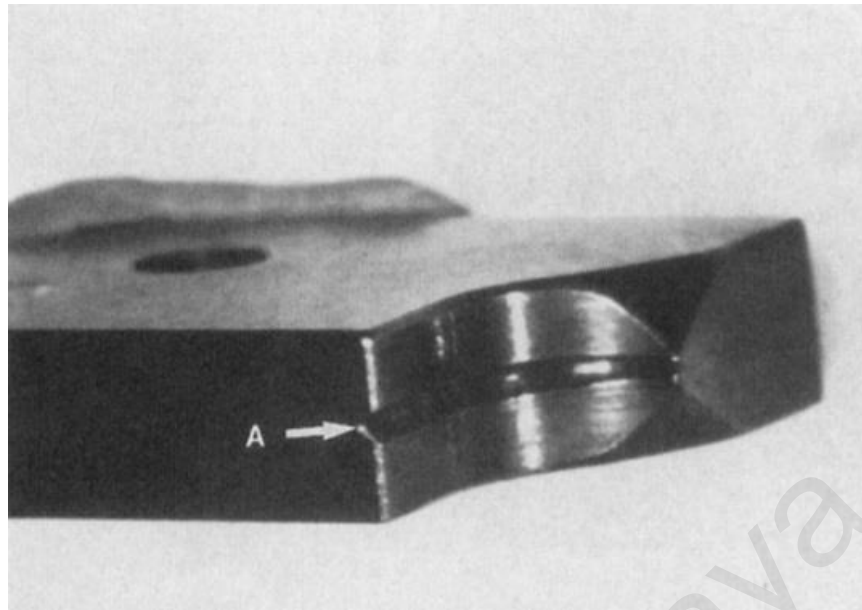


**Figure 3.9 The V-groove for guiding the instrument (Haikel *et al.*, 1999).**

### **3.5.5 Stainless Steel Block with Artificial Canal**

Larsen *et al.* (2009) tested instruments in a metal block with an artificial canal with a 60° angle of curvature and a 3-mm radius of curvature to the center of the 1.5-mm wide canal (Figure 3.10). An acrylic top face cover allowed for visualization of the files rotating in the canal and the removal of broken instruments between tests. A marker of permanent red ink was placed at 19 mm on the metal block to standardize instrument placement. The drawback of this design is the cylindrical canal grooved in the metal block was not able to constraint the instrument in a precise trajectory and that to insert the instruments at the same depth may be difficult. This will lead to inconsistent results.



**Figure 3.10 Metal block with 1.5 mm wide artificial canal (Larsen *et al.*, 2009).**

Plotino *et al.* (2006) manufactured an artificial canal that reproduced instrument size and taper (Figure 3.11), and this will ensure the instrument has a suitable trajectory. A copper duplicate of each instrument was milled and the original size of the instrument was increased by 0.1 mm using a computer numeric control machining bench (Bridgeport VMC 760XP3; Hardinge Machine Tools Ltd, Leicester, UK). This allowed the instrument to rotate freely inside the artificial canal during the test. The copper duplicates were constructed according to the curvature parameters that were chosen for the study. With these negative molds, the artificial canals were made using a die-sinking electrical-discharge machining process (Agiatron Hyperspark 3; AGIE Sa, Losone, Switzerland) in a stainless steel block. The blocks were hardened through annealing.

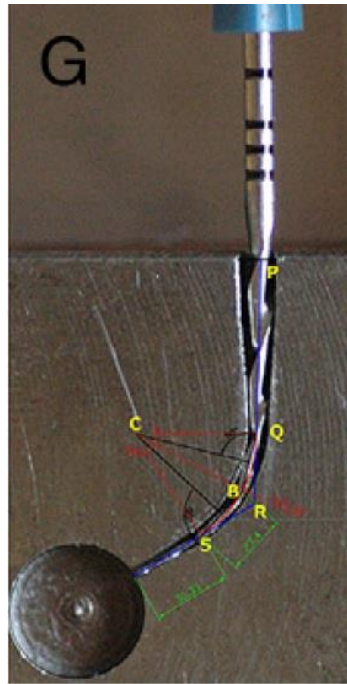


**Figure 3.11 An example of stainless steel block with artificial canal which reproduced the size and taper of instrument (Plotino *et al.*, 2009b).**

The artificial canal was covered with a tempered glass to prevent the instruments from slipping out and to allow for observation of the rotating instrument. Fracture was easily detectable because the instruments were visible through the glass window. To reduce the friction of the file as it contacted the artificial canal walls, a special high-flow synthetic oil designed for lubrication of mechanical parts was used.

The present device sought to overcome the limitations of other experimental designs in terms of the models used for testing. Each artificial canal was specifically designed for each instrument in terms of size and taper, giving it a precise trajectory.

## CHAPTER 4: MATERIALS AND METHODS

### 4.1 Sample Size Determination

The sample size was calculated using PS Power and Sample Size Calculations Software (Version 3.1.2). Based on the means and standard deviation of time to failure (in seconds) of WG ( $549.54 \pm 186.70$ ) and RB ( $872.06 \pm 155.40$ ) (Keskin *et al.*, 2017), the estimated sample size was ten (10) for each test group. This will provide 90% power at a significance level of 1% to reject the null hypothesis.

### 4.2 Pilot Study

A pilot study was conducted in order to determine the feasibility and practicality of the proposed study. The time to fracture of RB R25 and WG Primary at both temperature, the length of fractured tip and the SEM of fractured surface were evaluated.

In the pilot study, three RB R25 and three WG Primary instruments underwent the proposed cyclic fatigue resistance test at 20°C or at 35°C.

A custom made resin holder was used to place the fractured tips of each instruments during the SEM analysis to standardize the position in the SEM chamber. However, the images showed that debris were attached to the cross section surface of fractured instrument and the images were not ideal. This phenomenon was due to inadequate ultrasonic cleaning of fractured instruments prior SEM analysis. Thus, the ultrasonic cleaning duration of each instrument was extended to 20 minutes.

SEM magnification ranging from 30X to 2400X was used to analyze the cross section of fractured surface. After using multiple magnifications, magnification of 300X was decided as suitable to evaluate the whole fractured surface of tip.

### 4.3 Cyclic Fatigue Resistance Test

Twenty RB R25 (25/.08) and 20 WG Primary (25/.07) file each was inspected under a dental operating microscope at 20x magnification for morphologic analysis and signs of visible defect or irregularities. However, no defect was detected on all the instruments.

The cyclic fatigue test was carried out in a stainless steel artificial canal with a taper corresponding to the dimensions of the instruments tested. It simulates a root canal with 60° angle curvature and curvature radius of 5 mm. The curved segment of the canal was 5.24 mm in length (Figure 4.1a&b).

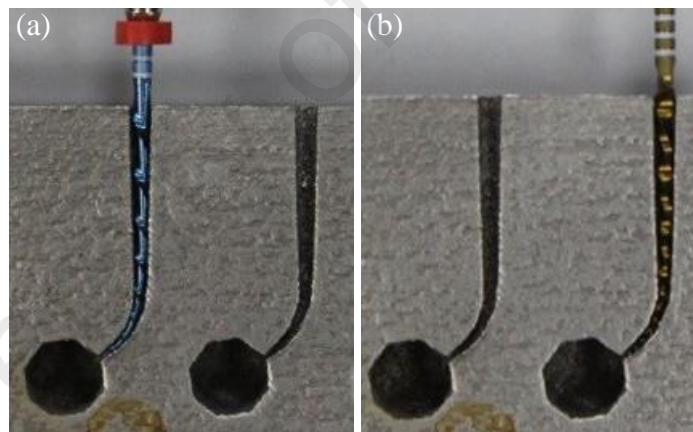


**Figure 4.1: (a) Stainless steel artificial canal which correspond to dimension of RB R25. (b) Stainless steel artificial canal which correspond to dimension of WG Primary.**

The stainless steel artificial canal was fix in a water bath which contained normal saline. Each instrument was introduced into the canal until the tip touched a shield at the end of the canal to standardize the instrument penetration depth (Figure 4.2a-e).

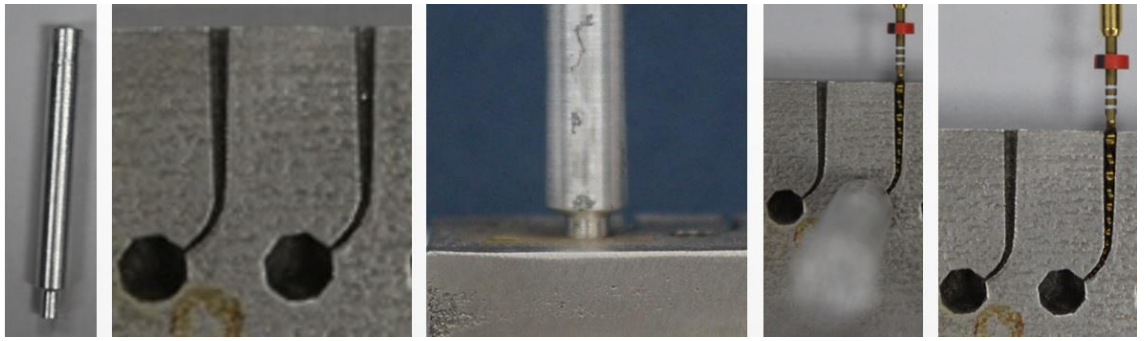


**Figure 4.2 (a) Shield. (b) Stainless steel canal. (c) Shield at the end of stainless steel canal. (d) Insertion of file. (e) Removal of shield.**

Ten instruments from each group were tested either at 20°C or at 35°C (Figure 4.3). The artificial canal was covered with tempered glass to prevent the instruments from slipping out. The temperature of the stainless steel artificial canal was monitored by a digital laser infrared temperature sensor (Figure 4.4).

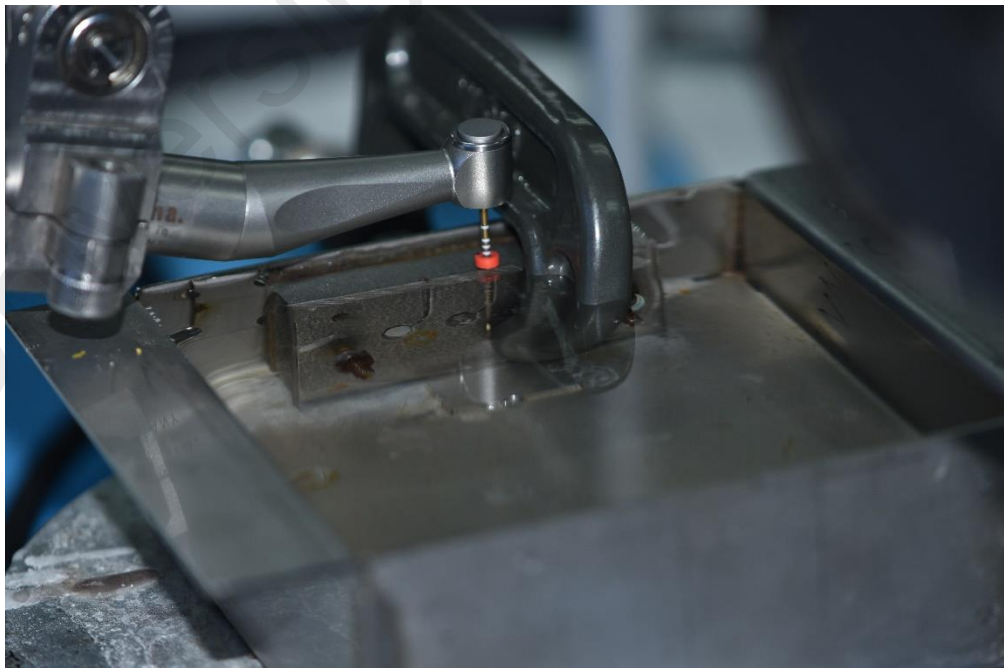


**Figure 4.3 Stainless steel canal in water bath.**





**Figure 4.4 Temperature of stainless steel canal monitored by digital laser infrared temperature sensor.**

Reciproc Blue R25 and WaveOne Gold Primary instruments were activated by using a 6:1 reduction handpiece (Sirona Dental Systems GmbH, Bensheim, Germany) which was powered by a torque-controlled motor (Silver; VDW GmbH) with proprietary movement (WaveOne ALL or Reciproc ALL).

The instruments reciprocate freely within the stainless steel canal. All instruments were activated until fracture. Time between commencement of the rotation and file fracture was taken. The instrument fracture was detected visually. The whole study was video recorded and cross checked later to minimize human errors. The length of the fractured tip was measured with digital micro-caliper (Figure 4.5) for each instrument in each group.



**Figure 4.5 Digital Micro-caliper.**

Two fractured files from each group were ultrasonic cleaned with ethanol absolute for 20 minutes prior being placed into a holder made with resin. After that, the files were examined under scanning electron microscopy (Quanta 250 FEG-SEM; FEI Company, USA) to determine the failure type of the Ni-Ti instruments. All images were taken under high vacuum with voltage set at 10.00kV with the magnification set at 300X.

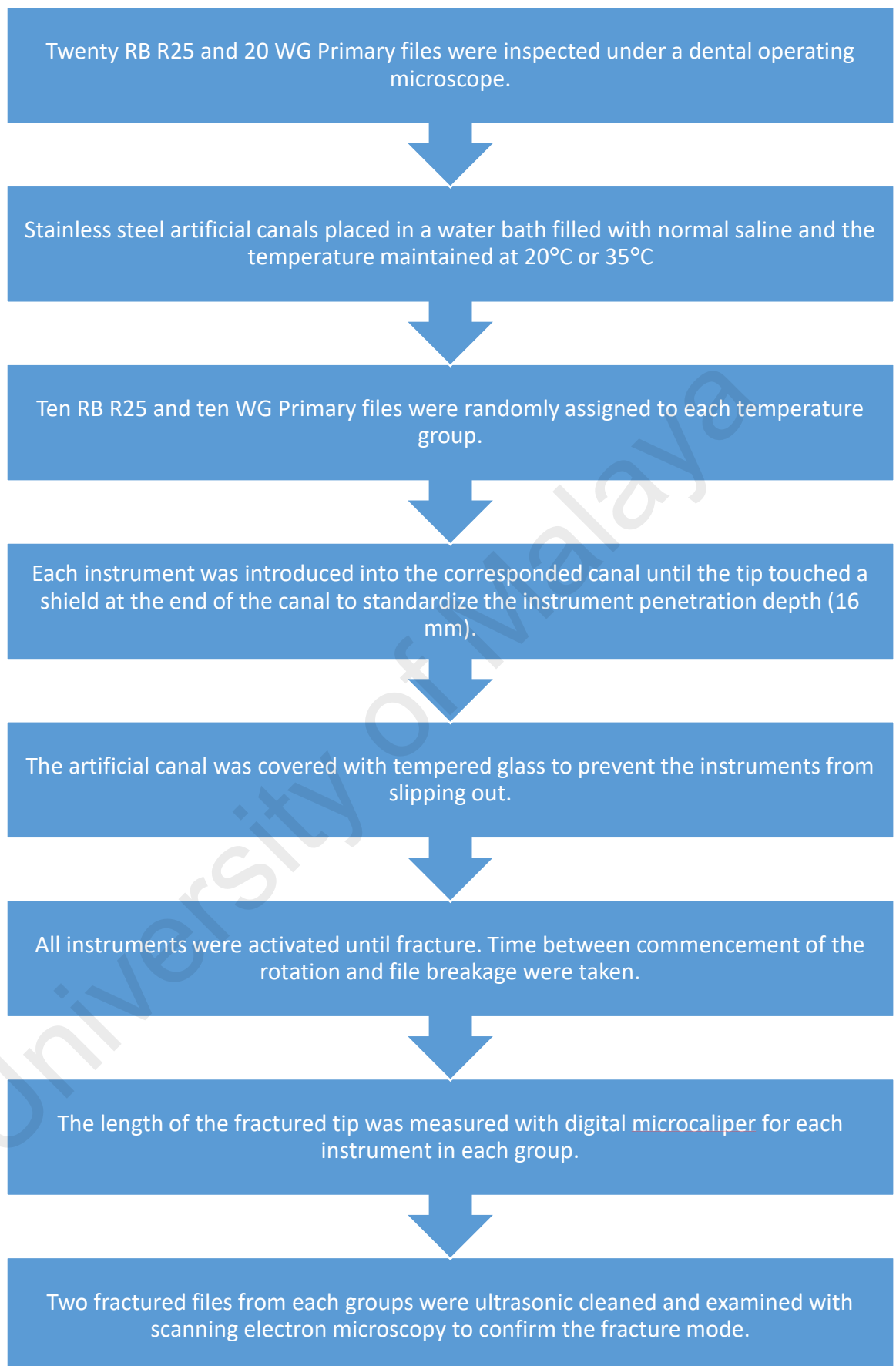


**Figure 4.6 Flow chart of the research methodology.**

#### **4.4 Data Analysis**

SPSS version 25 (SPSS Inc., Chicago, USA) was used to analyze the data. Two-way analysis of variance (ANOVA) and Bonferroni Post Hoc test were used to compare the time to failure of same system at the 2 different temperatures, the time to failure (in seconds) of different system at the same temperature and the length of the fractured fragments. The level of significance was set at  $\alpha=0.01$ .

University of Malaya

## CHAPTER 5: RESULTS

### 5.1 Length of Fractured Tip

The mean length of fractured tip of RB R25 at 20°C and 35°C was 4.17±0.49 mm and 3.87±0.63 mm respectively. The mean length of fractured tip of WG Primary at 20°C and 35°C are 3.97±0.24 mm and 3.82±0.28 mm respectively (Table 5.1).

**Table 5.1 Mean and SD of length of fractured tip of RB R25 and WG Primary at 20°C and 35°C.**

<b>Instrument</b>	<b>Temperature</b>	<b>Mean</b>	<b>SD</b>
<b>RB R25</b>	20°C	4.17	0.49
	35°C	3.87	0.63
<b>WG Primary</b>	20°C	3.97	0.24
	35°C	3.82	0.28

To evaluate the effect of two type of instruments (RB and WG) and two different temperatures (20°C and 35°C) on length of fractured tip, data were analysed based on Two-way ANOVA. Prior to data analysis, all variables were subjected to normality test and the results showed that all length of fractured tip were distributed normally (Table 5.2).

**Table 5.2 Normality test for length of fractured tip of RB and WG at 20°C and 35°C.**

	<b>Type</b>	<b>Statistic</b>	<b>df</b>	<b>p value</b>
<b>Length</b>	RB 20°C	0.87	10	0.09
	RB 35°C	0.93	10	0.44
	WG 20°C	0.95	10	0.64
	WG 35°C	0.89	10	0.18

*Shapiro-Wilk test*

The results of Two-way ANOVA (Table 5.3) showed that the effect of type of instrument yielded a F ratio of  $F(1,36) = 0.83$ ,  $p=0.37$ ,  $\eta^2=0.02$  and temperature yielded a F ratio of  $F(1,36) = 2.75$ ,  $p=0.11$ ,  $\eta^2=0.07$  and both were not statistically significant on length of fractured tip. The interaction between temperature and type of instrument was not significant,  $F(1,36) = 0.31$ ,  $p=0.58$ ,  $\eta^2=0.01$ .

**Table 5.3 Summary of Two-way ANOVA for temperature and type of instrument on length of fractured tip**

Source	SS	df	MS	F	p value	Partial Eta Square
<b>Instrument</b>	0.16	1	0.16	0.83	0.37	0.02
<b>Temperature</b>	0.53	1	0.53	2.75	0.11	0.07
<b>Instrument * temperature</b>	0.06	1	0.06	0.31	0.58	0.01

*Two-way ANOVA*

## 5.2 Time to Fracture

The mean time to fracture of RB R25 at 20°C and 35°C was 740.70±173.49 s and 326.90±85.95 s respectively. The mean length of fractured tip of WG Primary at 20°C and 35°C are 234.50±60.16 s and 205.00±30.06 s respectively (Table 5.4).

**Table 5.4 Mean and SD of time to fracture of RB R25 and WG Primary at 20°C and 35°C.**

Instrument	Temperature	Mean	SD
<b>RB R25</b>	20°C	740.70	173.49
	35°C	326.90	85.95
<b>WG Primary</b>	20°C	234.50	60.16
	35°C	205.00	30.06

To evaluate the effect of two type of instruments (RB and WG) and two different temperatures (20°C and 35°C) on time to fracture, data were analysed based on Two-way ANOVA. Prior to data analysis, all variables were subjected to normality test and the results showed that all time to fracture were distributed normally (Table 5.5).

**Table 5.5 Normality test for time to fracture of RB and WG at 20°C and 35°C.**

	Type	Statistic	df	<i>p</i> value
<b>Time</b>	RB 20°C	0.94	10	0.54
	RB 35°C	0.96	10	0.76
	WG 20°C	0.94	10	0.56
	WG 35°C	0.96	10	0.78

*Shapiro-Wilk test*

The results of Two-way ANOVA (Table 5.6) showed that the effect of type of instrument yielded a F ratio of  $F(1,36) = 93.92$ ,  $p < 0.001$ ,  $\eta^2 = 0.72$  and temperature yielded a F ratio of  $F(1,36) = 46.78$ ,  $p < 0.001$ ,  $\eta^2 = 0.57$  and both were statistically significant on time to fracture. The effect of interaction between temperature and type of instrument was statistically significant on time to fracture,  $F(1,36) = 35.16$ ,  $p < 0.001$ ,  $\eta^2 = 0.49$ .

**Table 5.6 Summary of Two-way ANOVA for temperature and type of instrument on length of fractured tip**

Source	SS	df	MS	F	<i>p</i> value	Partial Eta Square
<b>Instrument</b>	986274.03	1	986274.03	93.92	<0.001**	0.72
<b>Temperature</b>	491287.23	1	491287.23	46.78	<0.001**	0.57
<b>Instrument * temperature</b>	369216.23	1	369216.23	35.16	<0.001**	0.49

*Two-way ANOVA*

**\*\*significant at  $p < 0.01$**

To compare mean of time to fracture between the levels of instruments for each level of temperature, post hoc test (Bonferroni) was used. The results revealed that the difference between RB and WG at both 20°C and 35°C were significant ( $p < 0.001$ ) (Table 5.7).

**Table 5.7 The difference of time to fracture between levels of instruments for each level of temperature.**

Temperature	(I) Instrument	(J) Instrument	Mean Difference	SE	<i>p</i> value	Partial Eta Square
20°C	RB	WG	506.20	45.83	<0.001**	0.77
	WG	RB	-506.20	45.83	<0.001**	
35°C	RB	WG	121.90	45.83	<0.001**	0.62
	WG	RB	-121.90	45.83	<0.001**	

*Bonferroni test*

\*\*significant at  $p < 0.01$

To compare mean of time to fracture between the levels of temperatures for each level of instrument, post hoc test (Bonferroni) was used. The results revealed that the difference between 20°C and 35°C in RB was significant ( $p < 0.001$ ). However, there were not statistically significant ( $p > 0.05$ ) between 20°C and 35°C in WG (Table 5.8).

**Table 5.8 The difference of time to fracture between levels of temperatures for each level of instrument.**

Instrument	(I) Temp	(J) Temp	Mean Difference	SE	<i>p</i> value	Partial Eta Square
RB	20°C	35°C	413.80	45.83	<0.001**	0.69
	35°C	20°C	-413.80	45.83	<0.001**	
WG	20°C	35°C	29.50	45.83	0.52	0.01
	35°C	20°C	-29.50	45.83	0.52	

*Bonferroni test*

\*\*significant at  $p < 0.01$



### 5.3 Mode of Fracture

Fractographic examination was used to identify features on the fractured surface that would indicate the origin and direction of propagation of the crack(s) leading to material failure. The SEM images of the fracture surface (Figure 5.1 to Figure 5.4) showed typical feature of cyclic fatigue failure in all the tested instruments. These include crack initiation origin, surface pattern with fast fracture zone with dimples and fatigue striations.

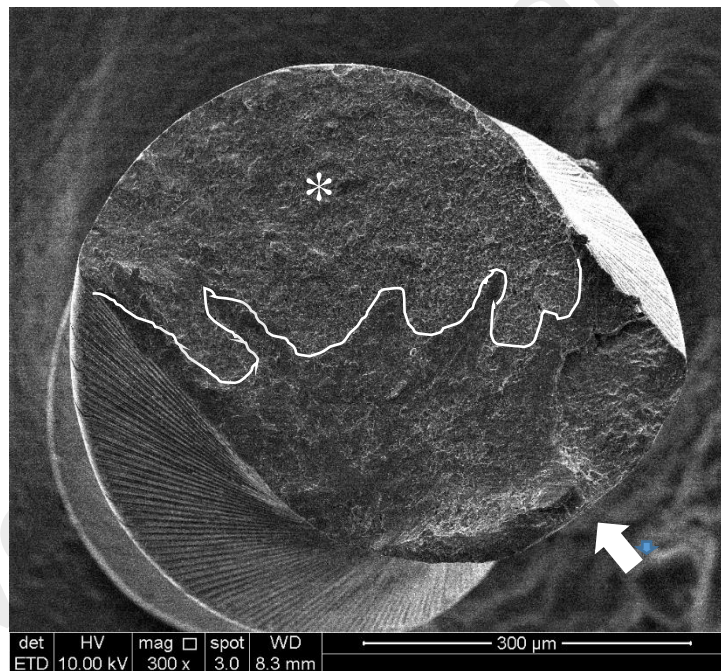


**Figure 5.1 SEM of RB R25 at 20°C with crack initiation origin (arrow) and fast fracture zone (asterisk) with dimples and fatigue striations.**

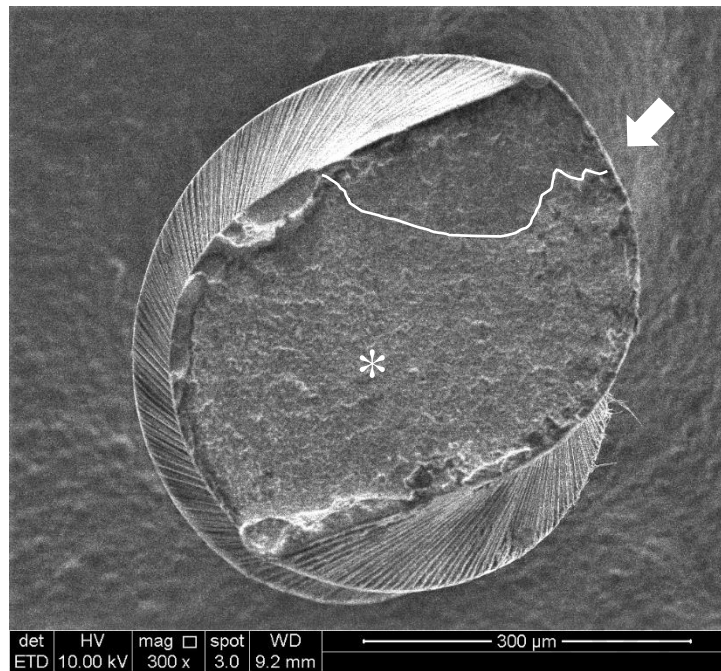


**Figure 5.2 SEM of RB R25 at 35°C with crack initiation origin (arrow) and fast fracture zone (asterisk) with dimples and fatigue striations.**

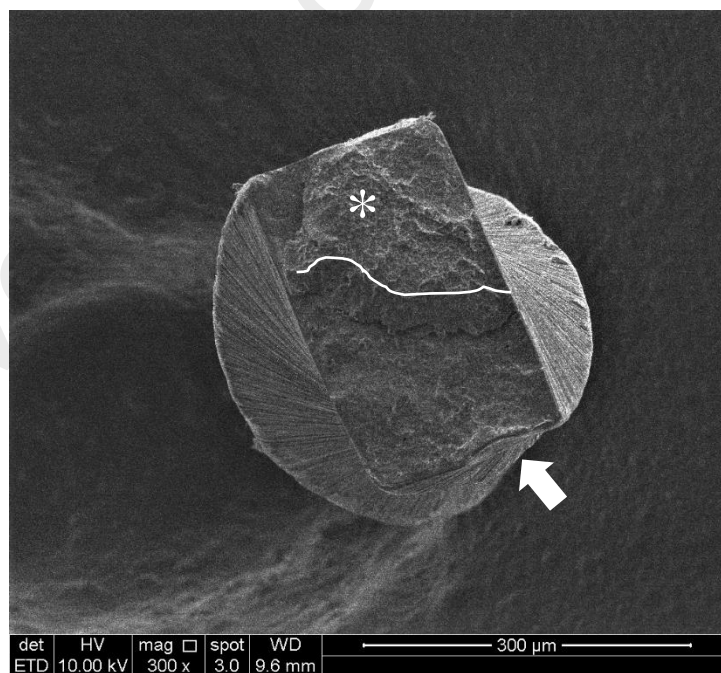


**Figure 5.3 SEM of WG Primary at 20°C with crack initiation origin (arrow) and fast fracture zone (asterisk) with dimples and fatigue striations.**

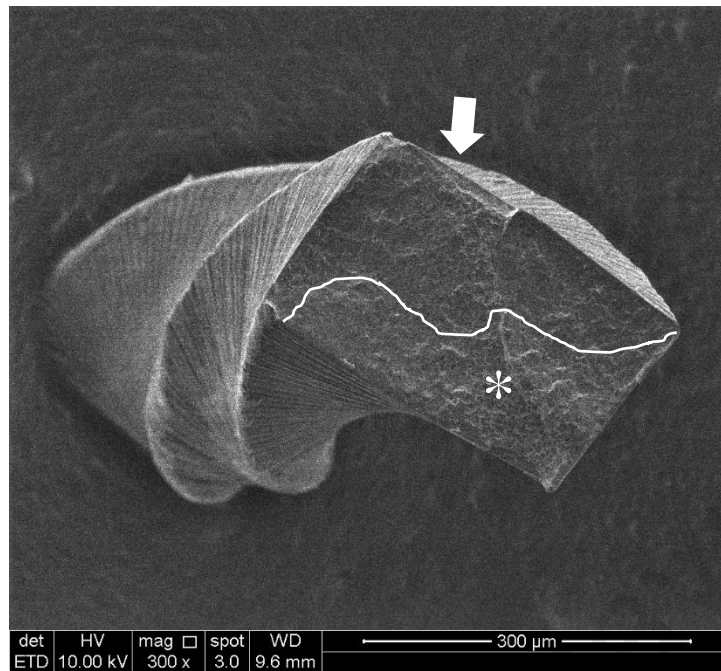


**Figure 5.4 SEM of WG Primary at 35°C with crack initiation origin (arrow) and fast fracture zone (asterisk) with dimples and fatigue striations.**

University of Malak

## CHAPTER 6: DISCUSSION

### 6.1 Methodology

The artificial canals were constructed with dimensions very close to those of the tested instrument to eliminate the slight changes in instrument positioning that can influence time to fracture. This was designed to make sure the precise trajectory of the files while reciprocating in the artificial canal and provide reproducible and accurate results (Plotino *et al.*, 2009b). If the instrument fits loosely in a canal, the description of the radius of curvature in those studies was likely to be overstated and the file was actually bent less severely than reported (Plotino *et al.*, 2009a).

An artificial canal with a 60° curvature angle and a 5-mm curvature radius was used in this study because most of the cyclic fatigue studies are based on these dimensions, thus this will facilitate the comparison between studies (Klymus *et al.*, 2018; Plotino *et al.*, 2017; Shen *et al.*, 2018).

The time to fracture has been used in the present study to evaluate the fatigue life of the files instead of the NCF. In fact, the NCF cannot be rigorously determined for reciprocating files rotating in both clockwise and counterclockwise directions. (Fidler, 2014)

### 6.2 Length

There was no significant difference with respect to the length of the fractured file fragments for all the instruments tested at both temperatures tested ( $p>0.05$ ). This finding is in agreement with Keskin *et al.* (2017) and Plotino *et al.* (2018). This confirmed that the tested instruments were positioned correctly in the artificial canal

curvature and faced similar stress during the experiment, thus ensuring sufficient standardization.

### **6.3 Time to Fracture**

#### **6.3.1 20°C vs 35°C**

##### **6.3.1.1 Reciproc Blue R25**

According to the results of the present study, the time to fracture of RB R25 at 20°C ( $740.70 \pm 173.49$  s) is significant higher than at 35°C ( $326.90 \pm 85.95$  s). Numerous studies had reported that when increasing the environmental temperature, cyclic fatigue resistance of Ni-Ti instrument was reduced significantly, thus indicating environmental temperature will affect the fatigue life of Ni-Ti (Alfawaz *et al.*, 2018; de Vasconcelos *et al.*, 2016; Dosanjh *et al.*, 2017; Shen *et al.*, 2018).

The  $A_s$  and  $A_f$  of RB R25 are 27°C and 34°C respectively (Plotino *et al.*, 2018). This indicated that at room temperature (20°C), the RB is in martensitic phase because 20°C is lower than the  $A_s$  temperature (temperature of initial conversion from martensite to austenite) which is 27°C. At intracanal temperature (35°C), it is in austenitic phase as 35°C is higher than  $A_f$  temperature (temperature of complete conversion of martensite into austenite) which is 34°C. Alloys containing a higher percentage of martensite at ambient temperature are more resistant to cyclic fatigue (Elnaghy & Elsaka, 2016; Plotino *et al.*, 2014). As RB is in martensitic phase at 20°C and in austenitic phase at 35°C, thus its cyclic fatigue resistance of RB at 20°C is significantly higher than 35°C

### 6.3.1.2 WaveOne Gold Primary

This study revealed that there was no significant difference between time to fracture of WG Primary at 20°C and 35°C. This result is consistent with Plotino *et al.* (2017) who evaluated the cyclic fatigue resistance of ProTaper Gold S1 and F2 at room temperature (20°C) and intracanal temperature (35°C) with a 60° angle and 5-mm radius of curvature of artificial canal. They revealed that increase the environmental temperature from room temperature to intracanal temperature did not influence the cyclic fatigue resistance of ProTaper Gold. On the other hand, Alfawaz *et al.* (2018) reported that the cyclic fatigue resistance of ProTaper Gold F2 significantly reduced when the environmental temperature increased from 25°C to 37°C.

There is lack of information about  $A_s$  and  $A_f$  of WG instrument in literature. However, several studies revealed that the  $A_s$  and  $A_f$  ProTaper Gold F2 which undergoes the same thermomechanical treatment as WG are about 40°C and 50°C respectively (Hieawy *et al.*, 2015). This indicated that WG instrument is in martensitic phase at both 20°C and 35°C. Thus, the cyclic fatigue resistance had no significant difference at both temperature.

### 6.3.2 20°C and 35°C

In this study, the time to fracture of RB R25 at 20°C is  $740.70 \pm 173.49$  s and it is significantly different from WG Primary ( $234.50 \pm 19.02$  s). This finding is similar to Gündoğar and Özyürek (2017) and Keskin *et al.* (2017) who reported that the time to fracture of RB R25 is significantly higher than WG primary. Moreover, at 35°C, RB had significantly longer time to fracture than WG ( $p < 0.001$ ) and this result is corroborated by Klymus *et al.* (2018).

In the present study, both instruments were made by the same alloy produced with the same proprietary thermal treatment (Zupanc *et al.*, 2018). Thus, the different results between the instruments should not be related to their metallurgical behaviour. The time to fracture of RB was significant longer than WG might be related to the different in cross section design of both tested instruments. RB have an S-shaped cross sections whereas WG has parallelogram-shaped cross section. Ray *et al.* (2007) and Tripi *et al.* (2006) reported that the cross sectional of instrument will influence their cyclic fatigue resistance. However, there are some studies which revealed that cyclic fatigue resistance of nickel titanium rotary instruments were not affected by the cross section design (Cheung & Darvell, 2007c; de Melo *et al.*, 2002). Thus, more investigations are needed to study the effect of file's design on cyclic fatigue resistance of nickel titanium rotary instruments.

#### **6.4 Limitation**

Even with careful planning, this study still has some limitation. Same as other *in vitro* studies, this study cannot perfectly simulate the clinical scenario. Secondly, there is only one type of canal curvature and radius of curvature have been used whereas in daily practice, the canal curvature and radius of curvature vary between different canals.

## CHAPTER 7: CONCLUSION & RECOMMENDATION

### 7.1 Conclusion

Within the limitation of this study, it can be concluded that the cyclic fatigue resistance of RB is significantly reduced when the environmental temperature is increased from 20°C to 35°C. However, increasing environmental temperature from 20°C to 35°C does not affect the cyclic fatigue resistance of WG. RB showed significant better cyclic fatigue resistance than WG in both 20°C and 35°C.

### 7.2 Recommendations

It is recommended to test the cyclic fatigue resistance of endodontic rotary instrument in different curvatures for example double curvature in order to simulate various clinical situations. Besides, different types of files regardless of motion and design of cross section should be tested in order to identify files with better cyclic fatigue resistance.

Clinically, we recommend that in a curve canal, RB has superior cyclic fatigue resistance as compared to WG.



## REFERENCES

- Adıgüzel, M., & Capar, I. D. (2017). Comparison of Cyclic Fatigue Resistance of WaveOne and WaveOne Gold Small, Primary, and Large Instruments. *Journal of Endodontics*, 43(4), 623-627.
- Alcalde, M. P., Tanomaru-Filho, M., Bramante, C. M., Duarte, M. A. H., Guerreiro-Tanomaru, J. M., Camilo-Pinto, J., Só, M. V. R., & Vivan, R. R. (2017). Cyclic and torsional fatigue resistance of reciprocating single files manufactured by different nickel-titanium alloys. *Journal of Endodontics*, 43(7), 1186-1191.
- Alfawaz, H., Alqedairi, A., Alsharekh, H., Almuzaini, E., Alzahrani, S., & Jamleh, A. (2018). Effects of sodium hypochlorite concentration and temperature on the cyclic fatigue resistance of heat-treated nickel-titanium rotary instruments. *Journal of Endodontics*, 44(10), 1563-1566.
- Anderson, M. E., Price, J. W., & Parashos, P. (2007). Fracture resistance of electropolished rotary nickel–titanium endodontic instruments. *Journal of Endodontics*, 33(10), 1212-1216.
- Barbosa, F. O. G., Gomes, J. A. D. C. P., & de Araújo, M. C. P. (2008). Influence of electrochemical polishing on the mechanical properties of K3 nickel-titanium rotary instruments. *Journal of endodontics*, 34(12), 1533-1536.
- Buehler, W. J., Gilfrich, J., & Wiley, R. (1963). Effect of low-temperature phase changes on the mechanical properties of alloys near composition TiNi. *Journal of Applied Physics*, 34(5), 1475-1477.
- Cheung, G., & Darvell, B. (2007a). Fatigue testing of a NiTi rotary instrument. Part 1: strain–life relationship. *International Endodontic Journal*, 40(8), 612-618.
- Cheung, G., & Darvell, B. (2007b). Fatigue testing of a NiTi rotary instrument. Part 2: fractographic analysis. *International Endodontic Journal*, 40(8), 619-625.
- Cheung, G., & Darvell, B. (2007c). Low - cycle fatigue of NiTi rotary instruments of various cross - sectional shapes. *International Endodontic Journal*, 40(8), 626-632.
- Cheung, G., Peng, B., Bian, Z., Shen, Y., & Darvell, B. (2005). Defects in ProTaper S1 instruments after clinical use: fractographic examination. *International Endodontic Journal*, 38(11), 802-809.
- Cheung, G. S., Shen, Y., & Darvell, B. W. (2007). Does electropolishing improve the low-cycle fatigue behavior of a nickel–titanium rotary instrument in hypochlorite?. *Journal of Endodontics*, 33(10), 1217-1221.
- De-Deus, G., Silva, E. J. N. L., Vieira, V. T. L., Belladonna, F. G., Elias, C. N., Plotino, G., & Grande, N. M. (2017). Blue thermomechanical treatment optimizes fatigue resistance and flexibility of the Reciproc files. *Journal of Endodontics*, 43(3), 462-466.

- De-Deus, G., Moreira, E., Lopes, H., & Elias, C. (2010). Extended cyclic fatigue life of F2 ProTaper instruments used in reciprocating movement. *International Endodontic Journal*, 43(12), 1063-1068.
- de Hemptinne, F., Slaus, G., Vandendael, M., Jacquet, W., De Moor, R. J., & Bottenberg, P. (2015). In vivo intracanal temperature evolution during endodontic treatment after the injection of room temperature or preheated sodium hypochlorite. *Journal of Endodontics*, 41(7), 1112-1115.
- de Melo, M. C. C., de Azevedo Bahia, M. G., & Buono, V. T. L. (2002). Fatigue resistance of engine-driven rotary nickel-titanium endodontic instruments. *Journal of Endodontics*, 28(11), 765-769.
- de Vasconcelos, R. A., Murphy, S., Carvalho, C. A. T., Govindjee, R. G., Govindjee, S., & Peters, O. A. (2016). Evidence for reduced fatigue resistance of contemporary rotary instruments exposed to body temperature. *Journal of Endodontics*, 42(5), 782-787.
- Dosanjh, A., Paurazas, S., & Askar, M. (2017). The effect of temperature on cyclic fatigue of nickel-titanium rotary endodontic instruments. *Journal of Endodontics*, 43(5), 823-826.
- Elnaghy, A., & Elsaka, S. (2016). Mechanical properties of ProTaper Gold nickel - titanium rotary instruments. *International Endodontic Journal*, 49(11), 1073-1078.
- Fidler, A. (2014). Kinematics of 2 reciprocating endodontic motors: the difference between actual and set values. *Journal of Endodontics*, 40(7), 990-994.
- Gambarini, G., Grande, N. M., Plotino, G., Somma, F., Garala, M., De Luca, M., & Testarelli, L. (2008). Fatigue resistance of engine-driven rotary nickel-titanium instruments produced by new manufacturing methods. *Journal of Endodontics*, 34(8), 1003-1005.
- Gambarini, G., Rubini, A. G., Al Sudani, D., Gergi, R., Culla, A., De Angelis, F., Di Carlo, S., Pompa, G., Osta, N., & Testarelli, L. (2012). Influence of different angles of reciprocation on the cyclic fatigue of nickel-titanium endodontic instruments. *Journal of Endodontics*, 38(10), 1408-1411.
- Gao, Y., Gutmann, J. L., Wilkinson, K., Maxwell, R., & Ammon, D. (2012). Evaluation of the impact of raw materials on the fatigue and mechanical properties of ProFile Vortex rotary instruments. *Journal of Endodontics*, 38(3), 398-401.
- Gao, Y., Shotton, V., Wilkinson, K., Phillips, G., & Johnson, W. B. (2010). Effects of raw material and rotational speed on the cyclic fatigue of ProFile Vortex rotary instruments. *Journal of Endodontics*, 36(7), 1205-1209.
- Gavini, G., Caldeira, C. L., Akisue, E., de Miranda Candeiro, G. T., & Kawakami, D. A. S. (2012). Resistance to flexural fatigue of Reciproc R25 files under continuous rotation and reciprocating movement. *Journal of Endodontics*, 38(5), 684-687.

- Gavini, G., Pessoa, O. F., Barletta, F. B., Vasconcellos, M. A. Z., & Caldeira, C. L. (2010). Cyclic fatigue resistance of rotary nickel-titanium instruments submitted to nitrogen ion implantation. *Journal of Endodontics*, 36(7), 1183-1186.
- Grande, N., Plotino, G., Pecci, R., Bedini, R., Malagnino, V., & Somma, F. (2006). Cyclic fatigue resistance and three - dimensional analysis of instruments from two nickel - titanium rotary systems. *International Endodontic Journal*, 39(10), 755-763.
- Grande, N. M., Ahmed, H. M. A., Cohen, S., Bukiet, F., & Plotino, G. (2015). Current assessment of reciprocation in endodontic preparation: a comprehensive review—part I: historic perspectives and current applications. *Journal of Endodontics*, 41(11), 1778-1783.
- Gündoğar, M., & Özyürek, T. (2017). Cyclic fatigue resistance of OneShape, HyFlex EDM, WaveOne gold, and Reciproc blue nickel-titanium instruments. *Journal of Endodontics*, 43(7), 1192-1196.
- Haikel, Y., Serfaty, R., Bateman, G., Senger, B., & Allemann, C. (1999). Dynamic and cyclic fatigue of engine-driven rotary nickel-titanium endodontic instruments. *Journal of Endodontics*, 25(6), 434-440.
- Hieawy, A., Haapasalo, M., Zhou, H., Wang, Z. J., & Shen, Y. (2015). Phase transformation behavior and resistance to bending and cyclic fatigue of ProTaper Gold and ProTaper Universal instruments. *Journal of Endodontics*, 41(7), 1134-1138.
- Higuera, O., Plotino, G., Tocci, L., Carrillo, G., Gambarini, G., & Jaramillo, D. E. (2015). Cyclic fatigue resistance of 3 different nickel-titanium reciprocating instruments in artificial canals. *Journal of Endodontics*, 41(6), 913-915.
- Jabbari, Y. S. A., Fehrman, J., Barnes, A. C., Zapf, A. M., Zinelis, S., & Berzins, D. W. (2012). Titanium nitride and nitrogen ion implanted coated dental materials. *Coatings*, 2(3), 160-178.
- Keskin, C., Inan, U., Demiral, M., & Keleş, A. (2017). Cyclic fatigue resistance of Reciproc Blue, Reciproc, and WaveOne Gold reciprocating instruments. *Journal of Endodontics*, 43(8), 1360-1363.
- Kiefner, P., Ban, M., & De-Deus, G. (2014). Is the reciprocating movement per se able to improve the cyclic fatigue resistance of instruments? *International Endodontic Journal*, 47(5), 430-436.
- Kim, H. C., Kwak, S. W., Cheung, G. S. P., Ko, D. H., Chung, S. M., & Lee, W. (2012). Cyclic fatigue and torsional resistance of two new nickel-titanium instruments used in reciprocation motion: Reciproc versus WaveOne. *Journal of Endodontics*, 38(4), 541-544.
- Kitchens Jr, G. G., Liewehr, F. R., & Moon, P. C. (2007). The effect of operational speed on the fracture of nickel-titanium rotary instruments. *Journal of Endodontics*, 33(1), 52-54.

- Klymus, M. E., Alcalde, M. P., Vivan, R. R., Só, M. V. R., de Vasconcelos, B. C., & Duarte, M. A. H. (2018). Effect of temperature on the cyclic fatigue resistance of thermally treated reciprocating instruments. *Clinical Oral Investigations*, 1-6.
- Kuhn, G., & Jordan, L. (2002). Fatigue and mechanical properties of nickel-titanium endodontic instruments. *Journal of Endodontics*, 28(10), 716-720.
- Larsen, C. M., Watanabe, I., Glickman, G. N., & He, J. (2009). Cyclic fatigue analysis of a new generation of nickel titanium rotary instruments. *Journal of Endodontics*, 35(3), 401-403.
- Li, U. M., Lee, B. S., Shih, C. T., Lan, W. H., & Lin, C. P. (2002). Cyclic fatigue of endodontic nickel titanium rotary instruments: static and dynamic tests. *Journal of Endodontics*, 28(6), 448-451.
- Lopes, H. P., Gambarra-Soares, T., Elias, C. N., Siqueira Jr, J. F., Inojosa, I. F., Lopes, W. S., & Vieira, V. T. (2013). Comparison of the mechanical properties of rotary instruments made of conventional nickel-titanium wire, M-wire, or nickel-titanium alloy in R-phase. *Journal of Endodontics*, 39(4), 516-520.
- Lopes, H. P., Moreira, E. J. L., Elias, C. N., de Almeida, R. A., & Neves, M. S. (2007). Cyclic fatigue of ProTaper instruments. *Journal of Endodontics*, 33(1), 55-57.
- McCormick, P. G., Liu, Y., & Miyazaki, S. (1993). Intrinsic thermal-mechanical behaviour associated with the stress-induced martensitic transformation in NiTi. *Materials Science and Engineering: A*, 167(1-2), 51-56.
- Nguyen, H. H., Fong, H., Paranjpe, A., Flake, N. M., Johnson, J. D., & Peters, O. A. (2014). Evaluation of the resistance to cyclic fatigue among ProTaper Next, ProTaper Universal, and Vortex Blue rotary instruments. *Journal of Endodontics*, 40(8), 1190-1193.
- Pedullà, E., Corsentino, G., Ambu, E., Rovai, F., Campedelli, F., Rapisarda, S., La Rosa, G., Rapisarda, E., & Grandini, S. (2018). Influence of continuous rotation or reciprocation of Optimum Torque Reverse motion on cyclic fatigue resistance of nickel - titanium rotary instruments. *International Endodontic Journal*, 51(5), 522-528.
- Pedullà, E., Grande, N. M., Plotino, G., Gambarini, G., & Rapisarda, E. (2013). Influence of continuous or reciprocating motion on cyclic fatigue resistance of 4 different nickel-titanium rotary instruments. *Journal of Endodontics*, 39(2), 258-261.
- Peng, B., Shen, Y., Cheung, G., & Xia, T. (2005). Defects in ProTaper S1 instruments after clinical use: longitudinal examination. *International Endodontic Journal*, 38(8), 550-557.
- Pereira, E. S., Gomes, R. O., Leroy, A. M., Singh, R., Peters, O. A., Bahia, M. G., & Bueno, V. T. (2013). Mechanical behavior of M-Wire and conventional NiTi wire used to manufacture rotary endodontic instruments. *Dental Materials*, 29(12), e318-e324.

- Pérez-Higueras, J. J., Arias, A., & José, C. (2013). Cyclic fatigue resistance of K3, K3XF, and twisted file nickel-titanium files under continuous rotation or reciprocating motion. *Journal of Endodontics*, 39(12), 1585-1588.
- Peters, O. A. (2004). Current challenges and concepts in the preparation of root canal systems: a review. *Journal of Endodontics*, 30(8), 559-567.
- Peters, O. A., & Barbakow, F. (2002). Dynamic torque and apical forces of ProFile. 04 rotary instruments during preparation of curved canals. *International Endodontic Journal*, 35(4), 379-389.
- Plotino, G., Grande, N., Testarelli, L., & Gambarini, G. (2012). Cyclic fatigue of Reciproc and WaveOne reciprocating instruments. *International Endodontic Journal*, 45(7), 614-618.
- Plotino, G., Grande, N. M., Bellido, M. M., Testarelli, L., & Gambarini, G. (2017). Influence of Temperature on Cyclic Fatigue Resistance of ProTaper Gold and ProTaper Universal Rotary Files. *Journal of Endodontics*, 43(2), 200-202.
- Plotino, G., Grande, N. M., Cordaro, M., Testarelli, L., & Gambarini, G. (2009a). Measurement of the trajectory of different NiTi rotary instruments in an artificial canal specifically designed for cyclic fatigue tests. *Oral Surgery, Oral Medicine, Oral Pathology, Oral Radiology, and Endodontology*, 108(3), e152-e156.
- Plotino, G., Grande, N. M., Cordaro, M., Testarelli, L., & Gambarini, G. (2009b). A review of cyclic fatigue testing of nickel-titanium rotary instruments. *Journal of Endodontics*, 35(11), 1469-1476.
- Plotino, G., Grande, N. M., Cotti, E., Testarelli, L., & Gambarini, G. (2014). Blue treatment enhances cyclic fatigue resistance of vortex nickel-titanium rotary files. *Journal of Endodontics*, 40(9), 1451-1453.
- Plotino, G., Grande, N. M., Sorci, E., Malagnino, V., & Somma, F. (2006). A comparison of cyclic fatigue between used and new Mtwo Ni-Ti rotary instruments. *International Endodontic Journal*, 39(9), 716-723.
- Plotino, G., Grande, N. M., Testarelli, L., Gambarini, G., Castagnola, R., Rossetti, A., Özyürek, T., Cordaro, M., & Fortunato, L. (2018). Cyclic Fatigue of Reciproc and Reciproc Blue Nickel-titanium Reciprocating Files at Different Environmental Temperatures. *Journal of Endodontics*, 44(10), 1549-1552.
- Praisarnti, C., Chang, J. W., & Cheung, G. S. (2010). Electropolishing Enhances the Resistance of Nickel-Titanium Rotary Files to Corrosion-Fatigue Failure in Hypochlorite. *Journal of Endodontics*, 36(8), 1354-1357.
- Pruett, J. P., Clement, D. J., & Carnes Jr, D. L. (1997). Cyclic fatigue testing of nickel-titanium endodontic instruments. *Journal of Endodontics*, 23(2), 77-85.
- Rapisardaa, E., Bonaccorsob, A., Tripib, T. R., Fragalkc, I., & Condorellid, G. G. (2000). The effect of surface treatments of nickel-titanium files on wear and cutting efficiency. *Oral Surgery, Oral Medicine, Oral Pathology, Oral Radiology, and Endodontology*, 89(3), 363-368.

- Ray, J. J., Kirkpatrick, T. C., & Rutledge, R. E. (2007). Cyclic fatigue of EndoSequence and K3 rotary files in a dynamic model. *Journal of Endodontics*, 33(12), 1469-1472.
- Roane, J. B., Sabala, C. L., & Duncanson Jr, M. G. (1985). The “balanced force” concept for instrumentation of curved canals. *Journal of Endodontics*, 11(5), 203-211.
- Sattapan, B., Nervo, G. J., Palamara, J. E., & Messer, H. H. (2000). Defects in rotary nickel-titanium files after clinical use. *Journal of Endodontics*, 26(3), 161-165.
- Schäfer, E. (2001). Shaping ability of Hero 642 rotary nickel-titanium instruments and stainless steel hand K-Flexofiles in simulated curved root canals. *Oral Surgery, Oral Medicine, Oral Pathology, Oral Radiology, and Endodontology*, 92(2), 215-220.
- Shen, Y., Huang, X., Wang, Z., Wei, X., & Haapasalo, M. (2018). Low environmental temperature influences the fatigue resistance of nickel-titanium files. *Journal of Endodontics*, 44(4), 626-629.
- Shen, Y., Qian, W., Abtin, H., Gao, Y., & Haapasalo, M. (2012). Effect of environment on fatigue failure of controlled memory wire nickel-titanium rotary instruments. *Journal of Endodontics*, 38(3), 376-380.
- Shen, Y., Zhou, H. M., Zheng, Y. F., Peng, B., & Haapasalo, M. (2013). Current challenges and concepts of the thermomechanical treatment of nickel-titanium instruments. *Journal of Endodontics*, 39(2), 163-172.
- Silva, E. J. N. L., Muniz, B. L., Pires, F., Belladonna, F. G., Neves, A. A., Souza, E. M., & De-Deus, G. (2016). Comparison of canal transportation in simulated curved canals prepared with ProTaper Universal and ProTaper Gold systems. *Restorative Dentistry & Endodontics*, 41(1), 1-5.
- Simon, S., Machtou, P., Tomson, P., Adams, N., & Lumley, P. (2008). Influence of fractured instruments on the success rate of endodontic treatment. *Dental Update*, 35(3), 172-179.
- Thompson, S. (2000). An overview of nickel–titanium alloys used in dentistry. *International Endodontic Journal*, 33(4), 297-310.
- Tripi, T. R., Bonaccorso, A., & Condorelli, G. G. (2006). Cyclic fatigue of different nickel-titanium endodontic rotary instruments. *Oral Surgery, Oral Medicine, Oral Pathology, Oral Radiology, and Endodontology*, 102(4), e106-e114.
- Tripi, T. R., Bonaccorso, A., Rapisarda, E., Tripi, V., Condorelli, G. G., Marino, R., & Fragalà, I. (2002). Depositions of nitrogen on NiTi instruments. *Journal of Endodontics*, 28(7), 497-500.
- Uygun, A. D., Kol, E., Topcu, M. K. C., Seekin, F., Ersoy, I., & Tanriver, M. (2016). Variations in cyclic fatigue resistance among ProTaper Gold, ProTaper Next and ProTaper Universal instruments at different levels. *International Endodontic Journal*, 49(5), 494-499.

- Walia, H., Brantley, W. A., & Gerstein, H. (1988). An initial investigation of the bending and torsional properties of Nitinol root canal files. *Journal of Endodontics*, 14(7), 346-351.
- Wan, J., Rasimick, B. J., Musikant, B. L., & Deutsch, A. S. (2011). A comparison of cyclic fatigue resistance in reciprocating and rotary nickel-titanium instruments. *Australian Endodontic Journal*, 37(3), 122-127.
- Wolle, C. F. B., Vasconcellos, M. A. Z., Hinrichs, R., Becker, A. N., & Barletta, F. B. (2009). The effect of argon and nitrogen ion implantation on nickel-titanium rotary instruments. *Journal of Endodontics*, 35(11), 1558-1562.
- Yared, G. (2008). Canal preparation using only one Ni-Ti rotary instrument: preliminary observations. *International Endodontic Journal*, 41(4), 339-344.
- Zhou, H., Peng, B., & Zheng, Y. F. (2013). An overview of the mechanical properties of nickel–titanium endodontic instruments. *Endodontic Topics*, 29(1), 42-54.
- Zupanc, J., Vahdat-Pajouh, N., & Schäfer, E. (2018). New thermomechanically treated NiTi alloys—a review. *International Endodontic Journal*, 51(10), 1088-1103.